

Excited State Relaxation Dynamics in Benzophenone and *meta*-Methyl Benzophenone Revealed by Time-Resolved Photoelectron Spectroscopy

Wenping Wu, Yukun Dan, Yuhuan Tian, Dongyuan Yang,* Guorong Wu,* and Xueming Yang



Cite This: *J. Phys. Chem. A* 2026, 130, 3006–3013



Read Online

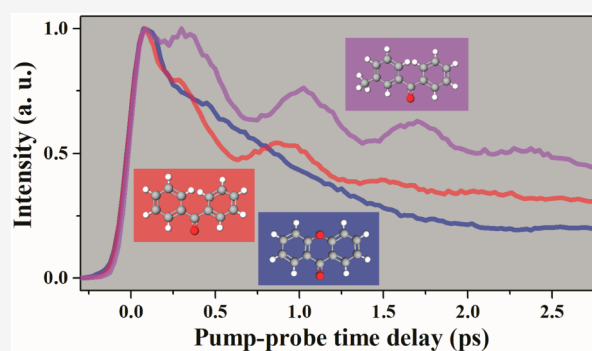
ACCESS |

Metrics & More

Article Recommendations

Supporting Information

ABSTRACT: The ultrafast electronic relaxation dynamics of benzophenone and *meta*-methyl benzophenone following photoexcitation in the ultraviolet range is investigated using the femtosecond time-resolved photoelectron spectroscopy method. At pump wavelengths of 267.6 and 241.0 nm, the optically bright $S_2(^1\pi\pi^*)$ state is directly excited and decays in 50 ± 10 fs via an efficient depopulation channel of internal conversion from the $S_2(^1\pi\pi^*)$ state to the $S_1(^1n\pi^*)$ state. Here, the subsequently populated $S_1(^1n\pi^*)$ state contains substantial excess vibrational energy, and its decay mechanism is tentatively proposed as the following: the wavepacket decays rapidly (in ~ 0.7 ps for benzophenone and ~ 1.4 ps for *meta*-methyl benzophenone) out of the Franck–Condon region on the $S_1(^1n\pi^*)$ state potential energy surface and probably bifurcates into two parts somewhere. One part undergoes ultrafast intersystem crossing to the $T_2(^3\pi\pi^*)$ state (and/or the $T_1(^3n\pi^*/^3\pi\pi^*)$ state), while the other further decays to the S_1 state minima. The remaining wavepacket evolves out of the S_1 state minima over a time constant of 6–20 ps and finally funnels down to the triplet manifold via intersystem crossing. In addition, methyl substitution effects and excitation energy dependence on the excited-state dynamics of benzophenone are also discussed. This experimental study provides valuable insights into the decay dynamics of photoexcited benzophenone.



1. INTRODUCTION

Benzophenone is widely utilized as a highly versatile photoinitiator since its unique photochemical properties enable efficient hydrogen abstraction, radical recombination and covalent cross-linking, making it indispensable in organic chemistry, biochemistry and material science.¹ Therefore, the photoinduced excited-state dynamics of benzophenone has been the subject of intensive theoretical studies over the past few decades.^{2–9} The $n\pi^*$ state mediated ultrafast intersystem crossing (ISC) to the triplet manifold occurs efficiently on a time scale of picoseconds in the cases of some types of ketone molecules, such as some α,β -enones^{10,11} and aromatic ketones.¹² In particular, benzophenone is also one of such prototypical molecules. Previously, Sergentu et al. performed high level *ab initio* calculations of benzophenone based on the CASPT2//CASSCF approach.² According to their computational results, they proposed that the $T_2(^3\pi\pi^*)$ state acts as an intermediate state between the $S_1(^1n\pi^*)$ state and the $T_1(^3n\pi^*)$ state (the T_1 state has a mixed $^3n\pi^*/^3\pi\pi^*$ character in the nonplanar case,^{2,13} so it can also be termed the $T_1(^3n\pi^*/^3\pi\pi^*)$ state) since a strong coupling between the S_1 and T_2 states was computed already in the Franck–Condon (FC) region. Furthermore, several surface hopping studies of the $S_1(^1n\pi^*)$ state decay dynamics of benzophenone were

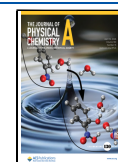
reported.^{3,4,8} Marazzi et al. performed the nonadiabatic dynamics simulations of gas-phase benzophenone, assuming a vertical $S_0 \rightarrow S_1$ transition.³ A subpicosecond decay of the S_1 state, together with ultrafast triplet (T_2 and T_1) population, was found within the first 600 fs. The lifetime of the S_1 state was estimated to be about 0.7 ps, while the fast dynamical equilibrium between T_1 and T_2 which exchange in just a few fs was proposed. In another simulation of the photodynamics of benzophenone for the first 20 ps after $n \rightarrow \pi^*$ excitation, Granucci and coworkers obtained an S_1 lifetime of about 16 ps by a monoexponential fit, or two lifetimes of 6 and 50 ps by a biexponential fit.⁴ Very recently, Kowalewski and coworkers performed the surface hopping calculations to study the excited-state dynamics of benzophenone, but they focused solely on the preceding internal conversion within the singlet manifold.⁸ Overall, according to previous theoretical investigations of benzophenone, both the direct ($S_1 \rightarrow T_1$) and

Received: January 26, 2026

Revised: March 28, 2026

Accepted: March 30, 2026

Published: April 6, 2026



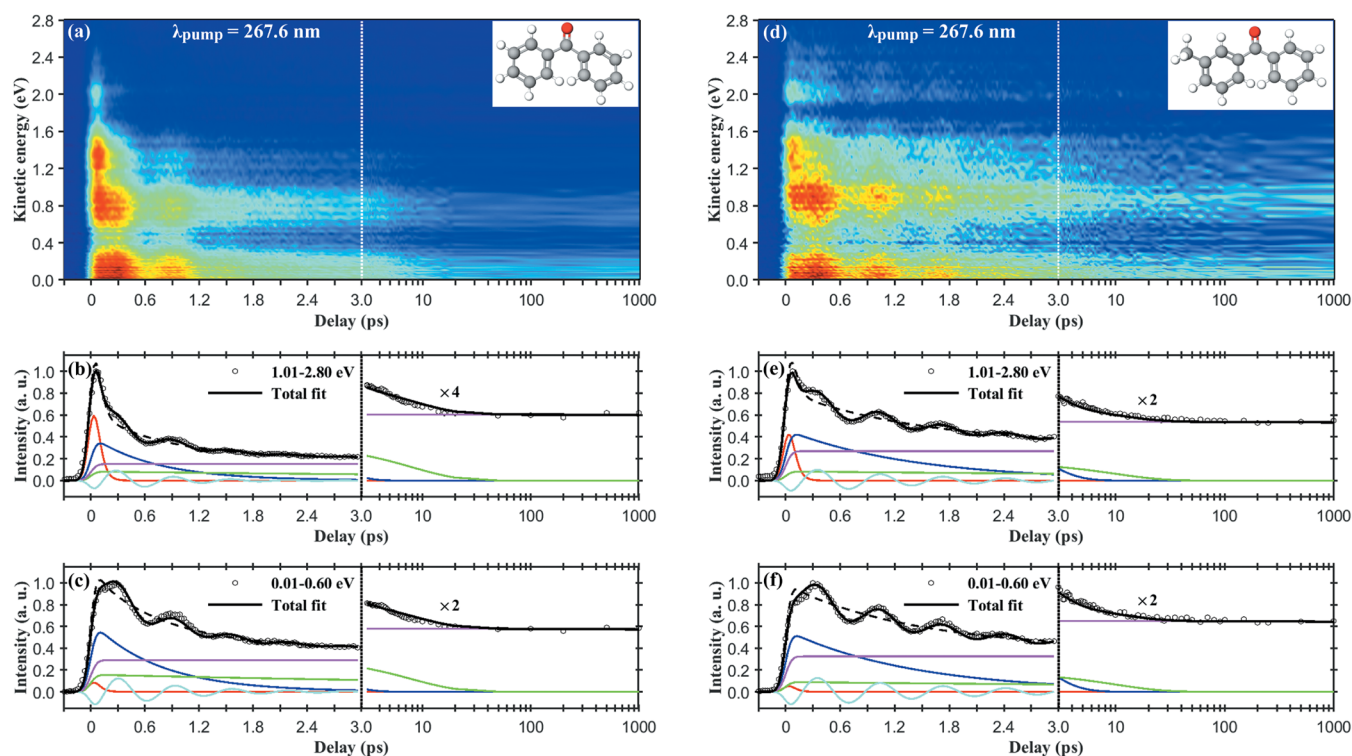


Figure 1. (a) TRPES spectrum of benzophenone upon excitation at 267.6 nm, after subtracting the background photoelectrons generated from single-color multiphoton ionization. Note that a combination of linear (≤ 3.0 ps) and logarithmic (≥ 3.0 ps) scales is used along the delay coordinate, as indicated by the vertical dotted line. A schematic structure of the benzophenone molecule is inset. (b, c) Normalized photoelectron transient derived by summing up the TRPES spectrum in (a) over the kinetic energy range of 1.01–2.80 and 0.01–0.60 eV, respectively. The dots represent the experimental data, while the solid lines show the fit to the experimental data. The dashed line represents the fit without the oscillatory component. A portion (≥ 3.0 ps) of it is scaled by a specific factor for better presentation. (d) Same as (a), but for *meta*-methyl benzophenone. (e, f) Same as (b, c), but for *meta*-methyl benzophenone.

indirect ($S_1 \rightarrow T_2 \rightarrow T_1$) mechanisms for the population of the lowest-lying triplet state are possible. However, which channel is prevalent has long been a matter of debate.^{2–4} Later on, this issue was also discussed in a review article.¹⁴ In more recent theoretical studies,^{6,7} the calculations of the ISC rate constants (k_{ISC}) clearly indicated that the indirect $S_1 \rightarrow T_2 \rightarrow T_1 \rightarrow S_0$ channel is the predominant decay pathway in benzophenone. The computed k_{ISC} value for the $S_1 \rightarrow T_2$ channel is much larger than that for the $S_1 \rightarrow T_1$ channel at the theoretical level.

So far, experimental studies on the excited-state dynamics of gas-phase benzophenone and its derivatives have rarely been reported, particularly those using direct time-resolved ultrafast spectroscopic methods. Previously, femtosecond and nanosecond pump–probe experiments on benzophenone were performed by Soep and coworkers.¹⁵ The nanosecond/submicrosecond pump–probe measurement clearly revealed a single exponential decay of 400 ± 50 ns for the free benzophenone molecule after excitation at 266 nm, which was reasonably assigned to the deactivation of the subsequently populated triplet state, $T_1(^3n\pi^*)$. Their femtosecond pump–probe experiments were carried out on a laser repetition rate of 20 Hz, while the 400 or 800 nm detection was utilized. Two different time constants (150 fs and 5 ps) were derived from the fit to their experimental results, together with the observation of oscillations with a period of about 550 fs.

The time-resolved study of gas-phase benzophenone¹⁵ preceded the aforementioned theoretical investigations, which commented on the experimental observations. However, in our opinion, the relaxation dynamics of the $S_1(^1n\pi^*)$ state in

benzophenone lacks a reasonable discussion or interpretation based on a combination of experimental findings and theoretical calculation results. For example, the lifetime and the depopulation mechanism of the $S_1(^1n\pi^*)$ state remain under debate. We are motivated by this puzzling issue and endeavor to achieve a more comprehensive picture of the deactivation mechanism of photoexcited benzophenone. Therefore, to gain more reliable experimental findings, in this work, we present a $[1 + 2']$ femtosecond time-resolved photoelectron spectroscopy (fs-TRPES) study on isolated benzophenone and also one of its alkyl-substituted derivatives, *meta*-methyl benzophenone.

2. EXPERIMENTAL METHODS

The $[1 + 2']$ fs-TRPES experiments were performed on a velocity map imaging (VMI) spectrometer.¹⁶ The detailed experimental methods have been described in our earlier publications.^{17,18} Herein, only some key features are given. Briefly, to generate jet-cooled molecular beam, a solid sample of benzophenone was heated to ~ 150 °C (~ 80 °C for a liquid sample of *meta*-methyl benzophenone) and mixed with helium carrier gas and expanded supersonically via a pulsed Even-Lavie valve operating at 1 kHz. The pump wavelengths were 267.6 nm (4.63 eV) and 241.0 nm (5.14 eV), while the probe laser was chosen at a fixed wavelength of 361.5 nm (3.43 eV) for two-photon ionization. A fine delay step of 25 fs was taken up to 2.5 ps. From 2.5 ps beyond, delay steps were larger and larger with a maximum delay of 1 ns employed. Thanks to the 1 kHz VMI spectrometer and femtosecond laser system employed here,¹⁶ the photoelectron images at each time delay were acquired by accumulating over millions of laser shots, after averaging hundreds of pump–probe scans. The 2D photoelectron images need to be

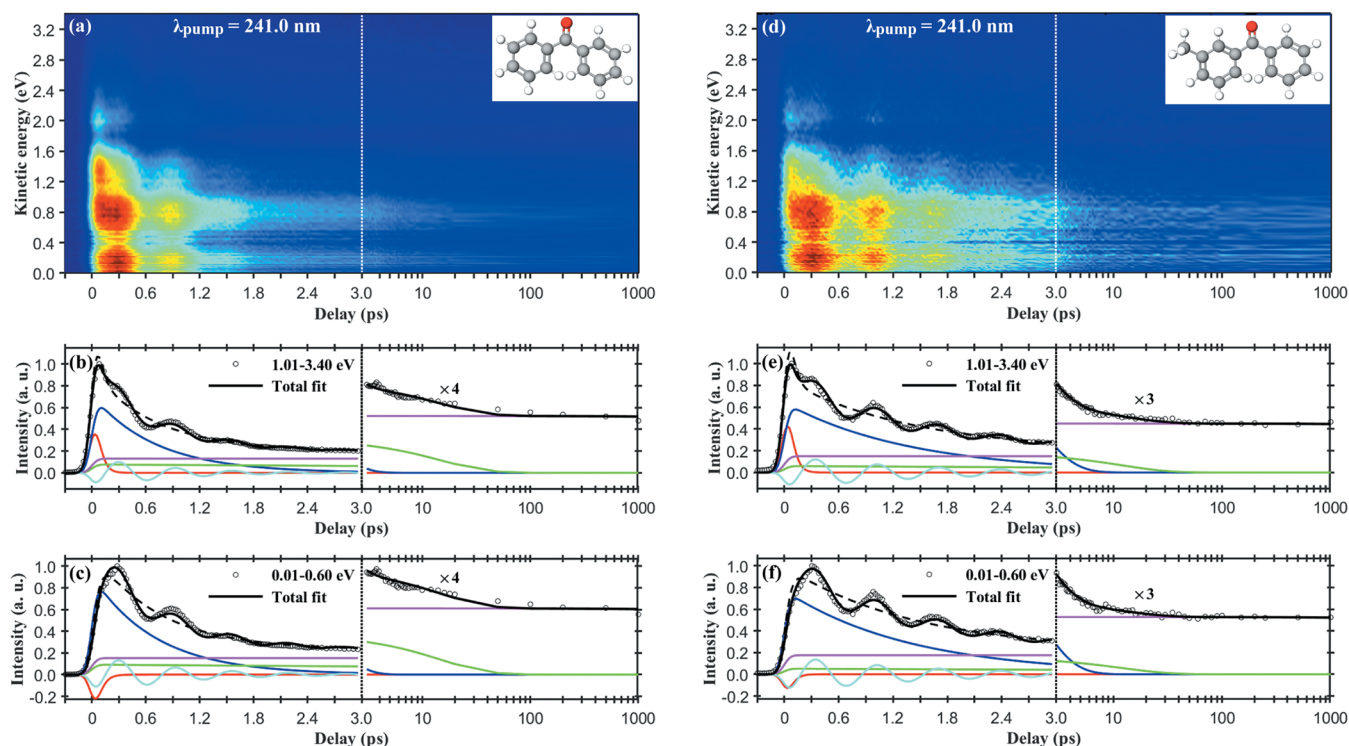


Figure 2. Same as Figure 1, but at a pump wavelength of 241.0 nm.

transferred to 3D distributions using the pBasex Abel inversion method.¹⁹ The time-dependent photoelectron 3D distributions were integrated along the recoiling angle to derive the photoelectron kinetic energy distributions, i.e., TRPES. Finally, the high-quality TRPES spectra were successfully obtained.

The two-color nonresonant ionization of NO molecules served to measure the time-zero and the cross-correlation (i.e., instrumental response function (IRF)) of the TRPES experiments. The [1 + 2'] IRFs were determined to be 130 ± 10 fs at full width at half-maximum (fwhm) based on the approximation that both pump and probe laser pulses were a Gaussian profile. The fluctuations in the time-zero and the uncertainties in the IRF were used to estimate the error bars of the derived time constants during the fits of the TRPES data.

3. RESULTS AND DISCUSSION

At a pump wavelength of 267.6 nm, the [1 + 2'] TRPES spectra of benzophenone and *meta*-methyl benzophenone are shown in Figure 1a and d, respectively, while the schematic structure of the corresponding molecule is inset. Note that a combination of linear (≤ 3.0 ps) and logarithmic (≥ 3.0 ps) scales is used along the time delay coordinate here, as indicated by the vertical dotted line. As revealed by visual inspection, the main feature of these two spectra is a dominant component that shows an extremely fast decay dynamics on a time scale of picosecond, together with a damped oscillation which nearly vanishes within 2 ps for benzophenone and 3 ps for *meta*-methyl benzophenone. It should be pointed out that the use of [1 + 2'] scheme in TRPES measurements is most likely to involve the resonance with Rydberg state(s) vibrational levels at the [1 + 1'] two-photon excitation energy in the probe step,^{20,21} resulting in different structures of the photoelectron kinetic energy distributions between the [1 + 1'] and the [1 + 2'] scheme TRPES spectra. Ionization from the Rydberg state vibrational levels to the cation is dominated by diagonal FC factors (the propensity rule of $\Delta\nu = 0$). As a consequence, the photoelectron kinetic energy distributions are reasonable to

show several peaks associated with different Rydberg states involved in two-photon ionization. This was also observed in our previous [1 + 2'] scheme TRPES spectra of other isolated molecules.^{22–24} Here the quantitative analysis of the photoelectron kinetic energy distributions is not provided, while the photoelectron transients at higher and lower kinetic energies are extracted and analyzed simultaneously, as shown in Figure 1b,c for benzophenone (Figure 1e,f for *meta*-methyl benzophenone). Normalized photoelectron transients derived by summing up the TRPES spectra over the whole kinetic energy range are presented in Figure S1 (see the Supporting Information).

In order to derive more detailed information about the values of the time constants, the oscillating period and the initial phase, a least-squares method was employed to simultaneously fit the photoelectron transients at higher and lower kinetic energies. The model used here can be described using multiexponential decay function along with an oscillatory component as the following expression:

$$\text{for } t \geq 0, \quad I(t) = A_{\text{osc}} \times \exp\left(-\frac{t}{\tau_{\text{osc}}}\right) \times \cos\left(\frac{2\pi t}{T} + \varphi_0\right) + \sum_{i=1}^n A_i \times \exp\left(-\frac{t}{\tau_i}\right)$$

$$\text{for } t < 0, \quad I(t) = 0 \quad (1)$$

Herein, t is the time delay and A_i represents the amplitude of the component associated with the τ_i time constant. A damped cosine function describes the oscillatory nature of the observed signal, while T is the oscillating period and φ_0 is the initial phase. The experimentally observed pump–probe signal should be a convolution of a Gaussian cross-correlation

Table 1. Pump Wavelengths Used, the Values of the Parameters in Eq 1 Derived from a Least-Squares Fit to the Corresponding Photoelectron Transients

Sample	Pump wavelength (λ_{pump})	Excited-state lifetimes (τ_i)			Period of oscillation (T)	Damping of oscillation (τ_{osc})	Phase of oscillation (φ_0/rad)	
		$S_2(^1\pi\pi^*)$	$S_1(^1n\pi^*)$	$T_1(^1n\pi^*)$				
benzophenone	267.6 nm	50 ± 10 fs	730 ± 30 fs	8 ± 2 ps	$\gg 1$ ns	630 ± 5 fs	730 ± 80 fs	3.14 ± 0.09
	241.0 nm	50 ± 10 fs	710 ± 30 fs	15 ± 5 ps	$\gg 1$ ns	630 ± 5 fs	850 ± 50 fs	3.23 ± 0.09
<i>meta</i> -methyl benzophenone	267.6 nm	50 ± 10 fs	1.40 ± 0.10 ps	10 ± 3 ps	$\gg 1$ ns	690 ± 5 fs	1.44 ± 0.11 ps	3.05 ± 0.09
	241.0 nm	50 ± 10 fs	1.40 ± 0.10 ps	12 ± 3 ps	$\gg 1$ ns	680 ± 5 fs	1.45 ± 0.10 ps	3.05 ± 0.09

function (i.e., instrumental response function (IRF)) and the decay of excited state population, $I(t)$. Herein, a numerical convolution approach is used²⁵ and describes the relative detection efficiency of the excited state²⁶ for a specific lifetime (τ_i) and a given value of the IRF (with a fwhm of 130 ± 10 fs in this work). An overall satisfactory fit to the experimental data was achieved using the aforementioned equation. Four different time constants (τ_1 , τ_2 , τ_3 and τ_4) were derived from the corresponding fit, together with other parameters in eq 1.

The [1 + 2'] TRPES spectra of benzophenone and *meta*-methyl benzophenone at a shorter pump wavelength (241.0 nm) are similar to those at 267.6 nm and presented in Figure 2, in which an analogous analysis can be performed and the fitting result is also shown. For the sake of comparison, all derived time constants (excluding their relative amplitudes, which are given in Table S1 in the Supporting Information) and the parameters of the oscillatory component at pump wavelengths of 267.6 and 241.0 nm for both molecules are summarized in Table 1.

Now we discuss the assignments of the derived time constants. As mentioned above, a lifetime of 400 ± 50 ns was experimentally measured for the T_1 state of benzophenone.¹⁵ Therefore, it is straightforward to assign the time constant of $\gg 1$ ns (i.e., τ_4) to the lifetime of the T_1 state. In the cases of benzophenone and *meta*-methyl benzophenone, the non-adiabatic relaxation from S_2 to S_1 begins at about 40 fs according to recent quantum dynamics simulations performed by Kowalewski and co-workers.^{8,27} They also concluded that the presence of a methyl group in the meta position does not significantly affect internal conversion from S_2 to S_1 . In contrast to the time evolution of the average adiabatic populations along the trajectories,⁸ the initially prepared $S_2(^1\pi\pi^*)$ state at pump wavelengths of 267.6 and 241.0 nm contains significant excess vibrational energy, thereby resulting in a slightly larger transition rate for the $S_2 \rightarrow S_1$ internal conversion process. Therefore, it is reasonable to assign the time constant of 50 ± 10 fs (i.e., τ_1) to the lifetime of the $S_2(^1\pi\pi^*)$ state. The ultrafast decay mechanism of the $S_2(^1\pi\pi^*)$ state in *meta*-methyl benzophenone is suggested to be similar to that in benzophenone. It should be emphasized that the relative detection efficiency of the S_2 state is actually much lower than that of the subsequently populated S_1 state. This is due to the limited time resolution of our pump–probe experiment. Here, the lifetime (50 ± 10 fs) of the S_2 state is close to the time resolution, which is roughly 1/4 of the value of the IRF (fwhm). Additionally, for a sequential kinetic process,²⁴ the amplitudes of the 50 ± 10 fs component should be associated with both the energy-resolved photoionization cross sections of the S_2 and S_1 states and can be negative at specific kinetic energies. Thus, as shown in Figure 1b,c,e,f and Figure 2b,c,e,f, the feature of the 50 ± 10 fs component

supports that the time constant of 50 ± 10 fs should be ascribed to the lifetime of the initially prepared excited state.

We note that the near degeneracy of $S_2(^1\pi\pi^*)$ and $S_3(^1\pi\pi^*)$ was taken into account in the surface hopping and quantum dynamics simulations by Kowalewski and coworkers.^{8,27} On the basis of their calculation results, the trajectories revealed a rapid exponential decay of the S_3 population to S_2 within the initial 10 fs of the dynamics, and the nonadiabatic relaxation is completed within 50 fs. According to the calculated UV spectra of benzophenone and *meta*-methyl benzophenone⁸ and a plausible vapor-phase excitation spectrum associated with $\pi^* \leftarrow \pi$ transitions of benzophenone,²⁸ we cannot totally rule out the contribution of the S_3 state in particular upon excitation at 241.0 nm. Actually, in Figure 2c,f, the fit does not adequately describe the experimental data within the first 300 fs. Due to the limited time resolution of the current pump–probe measurements, it is out of our capability to recognize the signal associated with the $S_3 \rightarrow S_2$ internal conversion channel. Moreover, for higher excitation energy (5.39 eV, ~ 230 nm), the $S_4(^1\pi\pi^*)$ state has the largest probability to be populated based on calculations of vertical excitation energies and oscillator strengths.^{2,9}

After photoexcitation, the population in S_2 is transferred to S_1 via internal conversion. Here, both the τ_2 and τ_3 time constants are tentatively assigned to the relaxation of the subsequently populated $S_1(^1n\pi^*)$ state, which contains substantial excess vibrational energy. It is not surprising that two time constants are observed for the $n\pi^*$ state, such as in the cases of pyrimidine nucleobases.²⁹ In general, this can be interpreted in terms of that either there are two dynamical processes for the $n\pi^*$ state, or its photoionization cross section is affected by structural or electronic variations (more details and the relevant kinetic model are given in the Supporting Information). Here we prefer to suggest that there are two relaxation pathways for the subsequently populated S_1 state. In the case of benzophenone, a value of ~ 0.7 ps is derived for τ_2 , which probably corresponds to a time scale of the initial geometry relaxation in the S_1 state. The wavepacket on the $S_1(^1n\pi^*)$ state potential energy surface evolves rapidly out of the FC region, immediately followed by efficient ISC to the $T_2(^3\pi\pi^*)$ state due to the non-negligible spin–orbit coupling and the small energy gap between the S_1 and T_2 states.^{2,4,6} At the FC geometry, S_1 is almost degenerate in energy with T_2 and T_3 (0.07 eV at the CASPT2 level³). Hence, there exists a favorable relaxation pathway from the FC region toward a region where the S_1 and T_2 are degenerate in energy, while reaching an S_1 minimum (and/or other seven isoenergetic local minima of the S_1 state⁹) is not expected to be predominant.^{2,3} Here the value of τ_2 is derived solely based on the fit to the experimental data and seems to match the subpicosecond S_1 lifetime obtained from one of the surface

hopping trajectory simulations,³ while τ_3 (6–20 ps) is responsible for the further decay of part of the wavepacket on the S_1 state surface. After leaving the FC region, a fraction of the wavepacket may evolve toward the S_1 local minima^{3,9} and finally decay more slowly before population transfer to the triplet manifold. The derived value of τ_3 at the pump wavelength of 267.6 nm is close to the lifetime of 5 ps observed in the previous TRPES measurement,¹⁵ while the value in the range of 6–20 ps is also reasonably consistent with the rate constant of the $S_1 \rightarrow T_2$ ISC process in several calculations.^{4,6,7} As revealed by theoretical determination of transition rate constants,⁷ the geometry relaxation of the subsequently populated S_1 state occurs faster than competitive ISCs at the S_0 geometry, while the $S_1 \rightarrow T_2$ ISC rate at the S_1 geometry matches the value of $1/\tau_3$. For benzophenone, the depopulation rate of the S_1 state is determined by the ISC process and may be vibrational-state dependent. According to the calculations of the ISC rate constant at the theoretical level, it was found that the number of normal modes may additionally enhance the rate constant of ISC of benzophenone.⁶ Here, we propose that $1/0.7 \text{ ps}^{-1}$ is an upper limit of the decay rate of the $S_1 \rightarrow T_2/T_1$ ISC processes for the S_1 state with substantial excess vibrational energy. This may explain the considerable population of the T_2 and T_1 states within 600 fs after excitation in the previous theoretical study of surface-hopping *ab initio* molecular dynamics of benzophenone.³ In other words, only part of the wavepacket evolves toward the minima of the S_1 state and finally decays with a lifetime of 6–20 ps. The proposed potential decay mechanism is shown schematically in Figure 3. An alternative explanation is that the

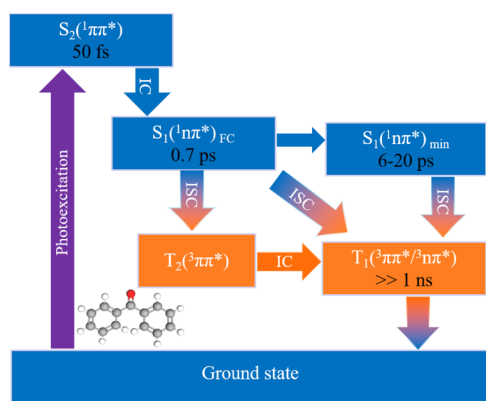


Figure 3. Schematic representation of the proposed potential decay mechanism of benzophenone.

presence of the T_2/S_1 intersystem recrossings may result in the repopulation of the S_1 state.² Then, the wavepacket is trapped around the S_1 state minima, leading to the second S_1 lifetime of 6–20 ps.

As presented in Table 1, within the margin of error, the derived time constants of τ_2 and τ_3 are almost identical at pump wavelengths of 267.6 and 241.0 nm since both excitation energies result in population of extremely high vibrational levels of the S_1 state via ultrafast $S_2 \rightarrow S_1$ internal conversion process. Moreover, methyl substitution effects on the excited-state dynamics of benzophenone are also discussed based on a comparison of the excited-state lifetimes. For *meta*-methyl benzophenone, the subsequently populated S_1 state undergoes slower geometry relaxation as compared to that in benzophenone (i.e., $\sim 1.4 \text{ ps}$ vs $\sim 0.7 \text{ ps}$). Overall, we propose

that the ultrafast electronic relaxation dynamics of *meta*-methyl benzophenone is similar to that of benzophenone.

It is worth mentioning that a vibrational quantum beat phenomenon was also clearly observed in all TRPES spectra. As mentioned above, identical wavepacket oscillations in the S_1 state of benzophenone have been previously observed and explained by Soep and coworkers.¹⁵ In brief, we agree with their interpretation that the wavepacket created along the phenyl torsional coordinates shows oscillations in the ionization efficiency as a function of the positions of the phenyl groups, resulting in a modulation in the photoelectron transients. Similar quantum beat phenomena associated with the coherent torsional motion were also observed in some ethylene-like molecules, such as tetrakis(dimethylamino)-ethylene.^{30,31} For benzophenone, the oscillating period is determined more accurately in this work, with the value of $630 \pm 5 \text{ fs}$. A period of 630 fs corresponds to a frequency of $\sim 53 \text{ cm}^{-1}$. As presented in Table 1, the oscillating period slightly increases in *meta*-methyl benzophenone due to the reduced wavenumber separation of the relevant beating vibrational states. All observed oscillations share a common initial phase of π (i.e., approximately 3.14) in the cosine function, within the margin of error in the fit. Strictly speaking, such periodic modulation should be described by a damped cosine function in combination with the exponential decay of the excited state population, ^{27–32} i.e.,

$$\left[\exp\left(-t/\tau_d\right) \times \cos\left(\frac{2\pi t}{T} + \varphi_0\right) \right] \times \exp\left(-t/\tau_i\right)$$
 while the damping time constant (τ_d) and the lifetime constant (τ_i) represent the dephasing of the coherence of the vibrational wavepacket and the decay of the excited electronic state, respectively. Here, we use a single exponential decay function (the time constant is labeled as τ_{osc}) to approximately describe the damping of the oscillation. The derived values of τ_{osc} are close to those of τ_2 , indicating that the dephasing lifetime (τ_d) is larger than the time scale (τ_2) of the evolution of the vibrational wavepacket on the S_1 state surface. In addition, according to the time evolution of some energetic and geometrical variables for the S_1 state, which was presented in the surface hopping study of excited state dynamics of benzophenone by Granucci and coworkers,⁴ one specific torsion-bending motion, i.e., a combination of the conrotatory torsion of phenyl rings and bending involving the carbonyl C atom (phenyl-C-phenyl angle opening), was found to be responsible for the oscillations in the TRPES spectra, with a period of about 600 fs. We also performed an additional TRPES experiment of xanthone, in which the relevant torsion-bending mode does not exist. The TRPES spectrum of xanthone upon excitation at 267.6 nm and the photoelectron transient are shown in Figure S2 (see the Supporting Information). The absence of oscillations in the decay strongly confirms their assignment.

The proposed vibrational coherence and ionization mechanism of benzophenone is schematically presented in Figure 4. For the ground state, the optimized molecular structure of isolated benzophenone is nonplanar. Specifically, according to an *ab initio* quantum mechanical calculation,³³ it was found that the twisted conformer is more stable than the planar one (the difference of free energies is 32 kJ/mol , i.e., 2675 cm^{-1}). In addition, the $C_1-C_7-C_{1'}$ (phenyl-C-phenyl) angle of the optimized geometry of the ground state (S_0) is 119.5° ³³ (119.8° ³⁴), while both of the two dihedral angles of the $C_6-C_1-C_7=O$ and $C_6-C_{1'}-C_7=O$ are 28.2° ³⁴. Meanwhile, the

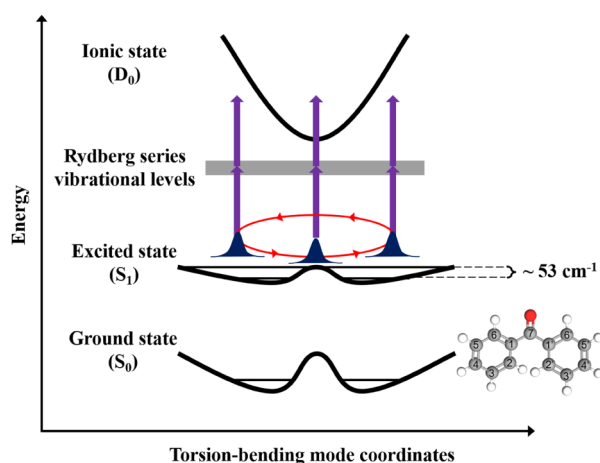


Figure 4. Schematic representation showing the proposed vibrational coherence and ionization mechanism of benzophenone.

optimized structure for the ground state of the benzophenone ion (D_0) was also calculated, yielding a $C_1-C_7-C_1'$ angle of 127.2° and the two aforementioned dihedral angles of 5.6° and 59.3° . Thus, the strong structural changes between the neutral and the ion were revealed by the calculation result. Moreover, the absence of a clear 0–0 transition in the single photoionization experiment of jet-cooled benzophenone also confirmed an apparent unfavorable FC overlap between the ground state neutral and the ground state ion.³⁴ Here, the $S_1(^1n\pi^*)$ state is subsequently populated via internal conversion from the optically bright $S_2(^1\pi\pi^*)$ state within about 50 fs. At the initial time (in the FC region or not far from it), the FC projection for the ionization of the $S_1(^1n\pi^*)$ state is poor and may not be efficient enough to reach the adiabatic energy of the ion. This is why the vibrational quantum beat phenomenon can be observed here and also explains an initial phase of π for the oscillations. As mentioned above, in the case of benzophenone, the wavenumber separation of two coherently excited vibrational states is observed to be $\sim 53 \text{ cm}^{-1}$. We note that the early fluorescence and phosphorescence excitation spectra exist a very long progression of $\sim 60 \text{ cm}^{-1}$ starting from the S_1 origin.^{35,36} The value of $\sim 60 \text{ cm}^{-1}$ was assigned to the frequency of the ring torsional mode. In particular, the phosphorescence excitation spectrum reveals that the frequency interval between the adjacent members of the progression decreases smoothly from 62.2 to 53.5 cm^{-1} with an increase in the vibrational quantum.³⁶ This is consistent with the wavenumber separation of $\sim 53 \text{ cm}^{-1}$ derived in this work, since the S_1 state is at extremely high vibrational levels.

The two-photon ionization mechanism in the probe step should be briefly discussed here. Note that the D_0 state of benzophenone has a strong n^{-1} character, while the D_1 and D_2 states are a mixing of n^{-1} and π^{-1} .³⁴ The adiabatic ionization energy for the ground state ion was measured to be $8.923 \pm 0.005 \text{ eV}$,³⁷ while those for the first and second excited states of the ion were tentatively suggested to be 9.17 ± 0.02 and $10.3 \pm 0.1 \text{ eV}$, respectively.³⁴ Therefore, at pump wavelengths of 267.6 and 241.0 nm, the $[1 + 2']$ three-photon energies are efficient for ionization to the D_0 , D_1 and D_2 states. As mentioned above, for all TRPES spectra, the photoelectron kinetic energy distributions show several similar peaks as well as broad band structures. This is likely to result from the combined effect of intermediate Rydberg state(s) and different

ionic states involved in the probe step. The relevant Rydberg series vibrational levels should match the $[1 + 1']$ two-photon excitation energies, as shown in Figure 4. Further discussion is beyond the scope of this work.

4. CONCLUSIONS

In conclusion, we have investigated the ultrafast decay dynamics of benzophenone and *meta*-methyl benzophenone upon excitation at 267.6 and 241.0 nm. Irradiation at these pump wavelengths prepares both molecules with high vibrational levels in the $S_2(^1\pi\pi^*)$ state which has a lifetime of $50 \pm 10 \text{ fs}$. The $S_1(^1n\pi^*)$ state with substantial excess vibrational energy is subsequently populated via efficient internal conversion from S_2 to S_1 since the S_2/S_1 conical intersection is apparently in the vicinity of the FC region. The wavepacket further evolves on the $S_1(^1n\pi^*)$ state surface and may undergo ultrafast ISC to the $T_2(^3\pi\pi^*)$ state (or involving a minor contribution from the higher-lying $T_3(^3\pi\pi^*)$ state) before reaching the minima of the S_1 state. The deactivation rate of the S_1 state is probably vibrational-state dependent. A fraction of the wavepacket is assumed to be trapped around the S_1 state minima and eventually ISC to the triplet manifold (T_2 and T_1) with a time scale of about 6–20 ps. Here, the indirect ($S_1 \rightarrow T_2 \rightarrow T_1$) mechanism is most likely to be the predominant decay channel for the S_1 state, while the direct ($S_1 \rightarrow T_1$) mechanism is not competitive for high vibrational levels of the S_1 state. Additionally, methyl substitution slows down the geometry relaxation in the S_1 state, with a characteristic time scale of $\sim 0.7 \text{ ps}$ for benzophenone and $\sim 1.4 \text{ ps}$ for *meta*-methyl benzophenone. Overall, compared with the previous similar study,¹⁵ the current $[1 + 2']$ fs-TRPES study on jet-cooled benzophenone and *meta*-methyl benzophenone presents the high-quality TRPES spectra, the analysis of which provides more quantitative information about the excited-state lifetimes of the S_2 and S_1 states, as well as the vibrational quantum beat. Our experimental result validates the earlier surface hopping calculations.^{3,4,8} To achieve a complete picture of the ultrafast electronic relaxation dynamics of benzophenone, further experimental and theoretical studies remain necessary. For example, a $[1 + 1']$ scheme TRPES experiment employing the vacuum ultraviolet probe laser and a time-resolved measurement with few-femtosecond temporal resolution are expected to provide deeper insights in the near future.

■ ASSOCIATED CONTENT

Supporting Information

The Supporting Information is available free of charge at <https://pubs.acs.org/doi/10.1021/acs.jpca.6c00528>.

Analysis of photoelectron transients of benzophenone and *meta*-methyl benzophenone, the TRPES spectrum of xanthone, details about the possible decay paths and the relevant kinetic model (PDF)

■ AUTHOR INFORMATION

Corresponding Authors

Dongyuan Yang – State Key Laboratory of Chemical Reaction Dynamics, Dalian Institute of Chemical Physics, Chinese Academy of Sciences, Dalian, Liaoning 116023, China; orcid.org/0000-0001-9525-7885; Email: yangdy@dicp.ac.cn

Guorong Wu – State Key Laboratory of Chemical Reaction Dynamics, Dalian Institute of Chemical Physics, Chinese Academy of Sciences, Dalian, Liaoning 116023, China;
✉ orcid.org/0000-0002-0212-183X; Email: wugr@dicp.ac.cn

Authors

Wenping Wu – State Key Laboratory of Chemical Reaction Dynamics, Dalian Institute of Chemical Physics, Chinese Academy of Sciences, Dalian, Liaoning 116023, China; University of Chinese Academy of Sciences, Beijing 100049, China

Yukun Dan – State Key Laboratory of Chemical Reaction Dynamics, Dalian Institute of Chemical Physics, Chinese Academy of Sciences, Dalian, Liaoning 116023, China; University of Chinese Academy of Sciences, Beijing 100049, China

Yuhuan Tian – State Key Laboratory of Chemical Reaction Dynamics, Dalian Institute of Chemical Physics, Chinese Academy of Sciences, Dalian, Liaoning 116023, China; University of Chinese Academy of Sciences, Beijing 100049, China

Xueming Yang – State Key Laboratory of Chemical Reaction Dynamics, Dalian Institute of Chemical Physics, Chinese Academy of Sciences, Dalian, Liaoning 116023, China; Department of Chemistry and Center for Advanced Light Source Research, College of Science, Southern University of Science and Technology, Shenzhen 518055, China;
✉ orcid.org/0000-0001-6684-9187

Complete contact information is available at:
<https://pubs.acs.org/10.1021/acs.jpca.6c00528>

Notes

The authors declare no competing financial interest.

ACKNOWLEDGMENTS

This experimental work was financially supported by the National Natural Science Foundation of China (grant nos. 22203095 and 22288201), the Natural Science Foundation of Liaoning Province (grant no. 2025-BS-0148), the Dalian Institute of Chemical Physics (grant no. DICP I202304), the State Key Laboratory of Molecular Reaction Dynamics (grant no. SKLMRD-Z202406), the National Key Research and Development Program of China (grant no. 2024YFF1500900), and the Key Technology Team of the Chinese Academy of Sciences (grant no. GJJSTD20220001). We also gratefully acknowledge the support and assistance provided by the Dalian Coherent Light Source (<https://cstr.cn/31127.02.DCLS>).

REFERENCES

(1) Dormán, G.; Nakamura, H.; Pulsipher, A.; Prestwich, G. D. The Life of Pi Star: Exploring the Exciting and Forbidden Worlds of the Benzophenone Photophore. *Chem. Rev.* **2016**, *116*, 15284–15398.
(2) Sergentu, D. C.; Maurice, R.; Havenith, R. W. A.; Broer, R.; Roca-Sanjuán, D. Computational Determination of the Dominant Triplet Population Mechanism in Photoexcited Benzophenone. *Phys. Chem. Chem. Phys.* **2014**, *16*, 25393–25403.
(3) Marazzi, M.; Mai, S.; Roca-Sanjuán, D.; Delcey, M. G.; Lindh, R.; González, L.; Monari, A. Benzophenone Ultrafast Triplet Population: Revisiting the Kinetic Model by Surface-Hopping Dynamics. *J. Phys. Chem. Lett.* **2016**, *7*, 622–626.

(4) Favero, L.; Granucci, G.; Persico, M. Surface Hopping Investigation of Benzophenone Excited State Dynamics. *Phys. Chem. Chem. Phys.* **2016**, *18*, 10499–10506.

(5) Segarra-Martí, J.; et al. Resolving the Singlet Excited State Manifold of Benzophenone by First-Principles Simulations and Ultrafast Spectroscopy. *J. Chem. Theory Comput.* **2018**, *14*, 2570–2585.

(6) Karak, P.; Chakrabarti, S. The Influence of Spin-Orbit Coupling, Duschinsky Rotation and Displacement Vector on the Rate of Intersystem Crossing of Benzophenone and Its Fused Analog Fluorenone: A Time Dependent Correlation Function Based Approach. *Phys. Chem. Chem. Phys.* **2020**, *22*, 24399–24409.

(7) Shizu, K.; Kaji, H. Theoretical Determination of Rate Constants from Excited States: Application to Benzophenone. *J. Phys. Chem. A* **2021**, *125*, 9000–9010.

(8) Restaino, L.; Schnappinger, T.; Kowalewski, M. Simulating Nonadiabatic Dynamics in Benzophenone: Tracing Internal Conversion through Photoelectron Spectra. *J. Chem. Phys.* **2025**, *162*, 084301.

(9) Flores-Larrañaga, R.; Castro, M. E.; Palma, A.; Melendez, F. J. Theoretical Insights of the Non-Rigid Behavior of Benzophenone by Franck-Condon Factors Approach. *Int. J. Quantum Chem.* **2025**, *125*, No. e70019.

(10) Schalk, O.; Schuurman, M. S.; Wu, G.; Lang, P.; Mucke, M.; Feifel, R.; Stolow, A. Internal Conversion Versus Intersystem Crossing: What Drives the Gas Phase Dynamics of Cyclic α , β -Enones? *J. Phys. Chem. A* **2014**, *118*, 2279–2287.

(11) Cao, J.; Xie, Z.-Z. Internal Conversion and Intersystem Crossing in α , β -Enones: A Combination of Electronic Structure Calculations and Dynamics Simulations. *Phys. Chem. Chem. Phys.* **2016**, *18*, 6931–6945.

(12) Alias-Rodríguez, M.; de Graaf, C.; Huix-Rotllant, M. Ultrafast Intersystem Crossing in Xanthone from Wavepacket Dynamics. *J. Am. Chem. Soc.* **2021**, *143*, 21474–21477.

(13) Wackerle, G.; Bar, M.; Zimmermann, H.; Dinse, K. P.; Yamauchi, S.; Kashmar, R. J.; Pratt, D. W. Optically Detected Magnetic Resonance Studies of Photoexcited ^{17}O -Benzophenone. Orbital Rotation in the Lowest Triplet State. *J. Chem. Phys.* **1982**, *76*, 2275–2292.

(14) Marian, C. M. Understanding and Controlling Intersystem Crossing in Molecules. *Annu. Rev. Phys. Chem.* **2021**, *72*, 617–640.

(15) Spighi, G.; Gaveau, M. A.; Mestdagh, J. M.; Poisson, L.; Soep, B. Gas Phase Dynamics of Triplet Formation in Benzophenone. *Phys. Chem. Chem. Phys.* **2014**, *16*, 9610–9618.

(16) He, Z.; Chen, Z.; Yang, D.; Dai, D.; Wu, G.; Yang, X. A New kHz Velocity Map Ion/Electron Imaging Spectrometer for Femto-second Time-Resolved Molecular Reaction Dynamics Studies. *Chin. J. Chem. Phys.* **2017**, *30*, 247–252.

(17) Yang, D.; Chen, Z.; He, Z.; Wang, H.; Min, Y.; Yuan, K.; Dai, D.; Wu, G.; Yang, X. Ultrafast Excited-State Dynamics of 2,4-Dimethylpyrrole. *Phys. Chem. Chem. Phys.* **2017**, *19*, 29146–29152.

(18) Feng, B.; Yang, D.; Min, Y.; Gao, Q.; Fang, B.; Wu, G.; Yang, X. Excitation Wavelength Dependent S_1 -State Decay Dynamics of 2-Aminopyridine and 3-Aminopyridine. *Phys. Chem. Chem. Phys.* **2023**, *25*, 17403–17409.

(19) Garcia, G. A.; Nahon, L.; Powis, I. Two-Dimensional Charged Particle Image Inversion Using a Polar Basis Function Expansion. *Rev. Sci. Instrum.* **2004**, *75*, 4989–4996.

(20) Song, J. K.; Tsubouchi, M.; Suzuki, T. Femtosecond Photoelectron Imaging on Pyrazine: Spectroscopy of 3s and 3p Rydberg States. *J. Chem. Phys.* **2001**, *115*, 8810–8818.

(21) Suzuki, T.; Wang, L.; Tsubouchi, M. Femtosecond Photoelectron Imaging on Pyrazine: (1 + 2') REMPI of Deuterated Pyrazine. *J. Phys. Chem. A* **2004**, *108*, 5764–5769.

(22) Wu, W.; Feng, B.; Tian, Y.; He, Z.; Yang, D.; Wu, G.; Yang, X. Insights into Ultrafast Relaxation Dynamics of Electronically Excited Furfural and 5-Methylfurfural. *J. Phys. Chem. A* **2024**, *128*, 8906–8913.

(23) Wu, W.; Tian, Y.; He, Z.; Yang, D.; Wu, G.; Yang, X. Investigation of Ultrafast Excited-State Dynamics of 3-Furfural. *Chin. J. Chem. Phys.* **2024**, *37*, 893–900.

(24) Feng, B.; Wu, W.; He, Z.; Yang, D.; Wu, G.; Yang, X. Ultrafast Decay Dynamics of the $2^1\pi\pi^*$ Electronic State of N-Methyl-2-Pyridone. *J. Phys. Chem. A* **2024**, *128*, 3840–3847.

(25) Feng, B.; Wu, W.; Yang, S.; He, Z.; Fang, B.; Yang, D.; Wu, G.; Yang, X. Insights into Ultrafast Decay Dynamics of Electronically Excited Pyridine-N-Oxide. *Phys. Chem. Chem. Phys.* **2024**, *26*, 8308–8317.

(26) Kotsina, N.; Townsend, D. Relative Detection Sensitivity in Ultrafast Spectroscopy: State Lifetime and Laser Pulse Duration Effects. *Phys. Chem. Chem. Phys.* **2017**, *19*, 29409–29417.

(27) Restaino, L.; Schnappinger, T.; Kowalewski, M. Simulation of Time-Resolved Site-Selective X-Ray Spectroscopy Tracing Non-adiabatic Dynamics in Meta-Methylbenzophenone. *Phys. Chem. Chem. Phys.* **2025**, *27*, 22725–22733.

(28) Itoh, T. Emission Characteristics of Benzophenone Vapor at Low Pressure. *J. Phys. Chem.* **1985**, *89*, 3949–3951.

(29) Miura, Y.; Yamamoto, Y.-I.; Karashima, S.; Orimo, N.; Hara, A.; Fukuoka, K.; Ishiyama, T.; Suzuki, T. Formation of Long-Lived Dark States During Electronic Relaxation of Pyrimidine Nucleobases Studied Using Extreme Ultraviolet Time-Resolved Photoelectron Spectroscopy. *J. Am. Chem. Soc.* **2023**, *145*, 3369–3381.

(30) Gloaguen, E.; Mestdagh, J. M.; Poisson, L.; Lepetit, F.; Visticot, J. P.; Soep, B.; Coroiu, M.; Eppink, A.; Parker, D. H. Experimental Evidence for Ultrafast Electronic Relaxation in Molecules, Mediated by Diffuse States. *J. Am. Chem. Soc.* **2005**, *127*, 16529–16534.

(31) Tian, Y.; Chen, Z.; Wu, W.; Wang, L.; He, Z.; Yang, D.; Wu, G.; Yang, X. A Time-, Angle- and Kinetic-Energy-Resolved Photoelectron Spectroscopic Study of Tetrakis(Dimethylamino)Ethylene. *Phys. Chem. Chem. Phys.* **2026**, *28*, 288–296.

(32) Yang, D.; Min, Y.; Feng, B.; Yang, X.; Wu, G. Vibrational-State Dependent Decay Dynamics of 2-Pyridone Excited to the S_1 Electronic State. *Phys. Chem. Chem. Phys.* **2022**, *24*, 22710–22715.

(33) Bezrodnaya, T. V.; Mel'nik, V. I.; Puchkovskaya, G. A.; Savranskii, L. I. Vibrational and Electronic Spectra of Benzophenone in Different Phase States: *Ab Initio* Calculations and Experiment. *J. Struct. Chem.* **2006**, *47*, 194–199.

(34) Khemiri, N.; Messaoudi, S.; Abderrabba, M.; Spighi, G.; Gaveau, M. A.; Briant, M.; Soep, B.; Mestdagh, J. M.; Hochlaf, M.; Poisson, L. Photoionization of Benzophenone in the Gas Phase: Theory and Experiment. *J. Phys. Chem. A* **2015**, *119*, 6148–6154.

(35) Holtzclaw, K. W.; Pratt, D. W. Prominent, and Restricted, Vibrational State Mixing in the Fluorescence Excitation Spectrum of Benzophenone. *J. Chem. Phys.* **1986**, *84*, 4713–4715.

(36) Kamei, S.; Sato, T.; Mikami, N.; Ito, M. n,π^* State of Jet-Cooled Benzophenone as Studied by Sensitized Phosphorescence Excitation Spectroscopy. *J. Phys. Chem.* **1986**, *90*, 5615–5619.

(37) Gouid, Z.; Röder, A.; Cunha de Miranda, B. K.; Gaveau, M.-A.; Briant, M.; Soep, B.; Mestdagh, J.-M.; Hochlaf, M.; Poisson, L. Energetics and Ionization Dynamics of Two Diarylketone Molecules: Benzophenone and Fluorenone. *Phys. Chem. Chem. Phys.* **2019**, *21*, 14453–14464.



CAS INSIGHTS™

EXPLORE THE INNOVATIONS SHAPING TOMORROW

Discover the latest scientific research and trends with CAS Insights. Subscribe for email updates on new articles, reports, and webinars at the intersection of science and innovation.

Subscribe today

CAS
A Division of the
American Chemical Society